HHS Public Access

Author manuscript

Toxicol Appl Pharmacol. Author manuscript; available in PMC 2021 November 15.

Published in final edited form as:

Toxicol Appl Pharmacol. 2020 November 15; 407: 115236. doi:10.1016/j.taap.2020.115236.

Fatty acid nitroalkenes inhibit the inflammatory response to bleomycin-mediated lung injury

Melissa L. Wilkinson[a,b], **Elena Abramova**[a,b], **Changjiang Guo**[a,b], **James G. Gow**[a,d], **Alexa Murray**[a,b], **Adolf Koudelka**[c], **Veronika Cechova**[c], **Bruce A. Freeman**[c], **Andrew J. Gow**[a,b]

[a.]Department of Pharmacology and Toxicology, Ernest Mario School of Pharmacy, The State University of New Jersey, 160 Frelinghuysen Road, Piscataway, NJ, 08854, USA

[b.]Environmental and Occupational Health Sciences Institute, Rutgers, The State University of New Jersey, 170 Frelinghuysen Road, Piscataway, NJ, 08854, USA

[c.]Department of Pharmacology and Chemical Biology, University of Pittsburgh School of Medicine, 3550 Terrace St, Pittsburgh, PA, 15213, USA

[d.]Dartmouth College, Hanover, NH, 03755, USA

Abstract

Fatty acid nitroalkenes are reversibly-reactive electrophiles, endogenously detectable at nM concentrations, displaying anti-inflammatory actions. Nitroalkenes like 9- or 10-nitro-octadec-9-enoic acid (e.g. nitro-oleic acid, OA-NO_2) pleiotropically suppress cardiovascular inflammatory responses, with pulmonary responses less well defined. C57BL/6J male mice were intratracheally administered bleomycin (3U/kg, ITB), to induce pulmonary inflammation and acute injury, or saline and were treated with 50μL OA-NO_2 (50μg) or vehicle in the same instillation and 72h post-exposure to assess anti-inflammatory properties. Bronchoalveolar lavage (BAL) and lung tissue were collected 7d later. ITB mice lost body weight, with OA-NO_2 mitigating this loss (−2.3±0.94 vs −0.4±0.83g). Histology revealed ITB induced cellular infiltration, proteinaceous debris deposition, and tissue injury, all significantly reduced by OA-NO_2. Flow cytometry analysis of BAL demonstrated loss of Siglec F^+/F4/80^+/$CD45^+$ alveolar macrophages with ITB (89±3.5 vs 30±3.7%). Analysis of CD11b/CD11c expressing cells showed ITB-induced non-resident

Corresponding Author: Andrew J. Gow, Department of Pharmacology and Toxicology, Ernesto School of Pharmacy, Rutgers, The State University of New Jersey, 160 Frelinghuysen Road, Piscataway, NJ 08854, Tel: (848)-445-4612, gow@pharmacy.rutgers.edu.

Credit Author Statement:

Melissa Wilkinson did the majority of the experimental work and wrote the first version of the manuscript. She has been responsible for all the editing work with regards to comments form co-authors etc.

Elena Abramova assisted with the ITB model and the administration of OA-NO_2. She was also a key element to the collection and preparation of samples as well as the assessment of BAL contents

Changjiang Guo assisted with the tissue preparation and cellular isolation and labeling James Gow & Alexa Murray both assisted with the conduct of the flow and its analysis as well as scoring histology sections

Adolf Koudelka and Veronika Cechova both assisted with PCR analysis, while Adolf also assisted in the preparation of the manuscript

Bruce Freeman supplied the OA-NO_2 and consulted on its use in a pulmonary injury model. He also edited and assisted in the preparation of the manuscript

Andrew Gow supervised the project and was responsible for the initial experimental design. He assisted in the interpretation of the flow data and the single cell western analysis. He edited the manuscript and is responsible for the final version

macrophage infiltration (4±2.3 vs 43±2.4%) was decreased by OA-NO_2 (24±2.4%). Additionally, OA-NO_2 attenuated increases in mature, activated interstitial macrophages (23±4.8 vs. 43±5.4%) in lung tissue digests. Flow analysis of $CD31^{-}/CD45^{-}/Sca\text{-}1^{+}$ mesenchymal cells revealed ITB increased $CD44^{+}$ populations (1±0.4 vs 4±0.4MFI), significantly reduced by OA-NO_2 (3±0.4MFI). Single cell analysis of mesenchymal cells by western blotting showed profibrotic ZEB1 protein expression induced by ITB. Lung digest $CD45^{+}$ cells revealed ITB increased $HMGB1^{+}$ cells, with OA-NO_2 suppressing this response. Inhibition of HMGB1 expression correlated with increased basal phospholipid production and SP-B expression in the lung lining. These findings indicate OA-NO_2 inhibits ITB-induced pro-inflammatory responses by modulating resident cell function.

Keywords

Nitro-oleic acid; nitroalkene; inflammation; acute lung injury; bleomycin; macrophage

Introduction

Acute lung injury (ALI) is a disorder characterized by pulmonary inflammation, predominantly through alterations in the innate immune response and endothelial and epithelial airway cell function (1,2). Clinical responses vary from dyspnea to acute respiratory distress syndrome (1). In turn, this contributes to substantial morbidity and mortality and, in patients with less severe ALI, permanently decreased lung function (3,4). ALI occurs as a result of exposure to a variety of inhaled toxicants and infectious agents There are limited therapies leading to adverse effects on quality of life (1).

Intratracheal administration of bleomycin (ITB) is a well-established model of ALI (5,6). ITB induces inflammation, loss of epithelial barrier function, and damage to the airway epithelium within 7d and consequent fibrosis (7–9). The inflammatory response to ITB occurs within the innate immune system and is macrophage dominant (5). Thus, ITB is a useful model for examining macrophage activation and phenotype in response to injury. Increased nitric oxide (NO) production is a key component in the inflammatory responses of the lung during acute macrophage activation, as evidenced by studies employing both a $NOS2^{-/-}$ murine model and NOS2 inhibitors (10). As nitro-fatty acids, such as nitro-oleic fatty acid (OA-NO_2), inhibit macrophage activation (11,12), we chose to examine the impact of OA-NO_2 on airway cell responses to ITB.

Due to its nature as a soft electrophile, OA-NO_2 has the ability to reversibly alkylate cysteine residues on proteins and other small molecules via Michael addition (13–16). OA-NO_2 reduces inflammation in several different models of metabolic and inflammatory disease via the modification of transcription factor and signal transduction pathway activities, as well as the direct inhibition of the catalytic activity of pro-inflammatory enzymes (17). In addition, OA-NO_2 has been shown to reduce macrophage activation in response to LPS and cigarette smoke (18,19). Nitroalkenes activate multiple anti-inflammatory transcriptional regulatory proteins such as Kelch-like ECH-associated protein 1/nuclear factor (erythroid-derived 2)-like 2 (Keap1/Nrf2) (20) and peroxisome proliferator-

activated receptor gamma (PPAR-γ) (21–23) and inhibit several pro-inflammatory signaling mechanisms regulated by nuclear factor kappa-light-chain-enhancer of activated B cells (NF-κB) (21), janus kinase/signal transducer and activator of transcription proteins (JAK/STAT) (24) and stimulator of interferon genes (STING) (25). All of these mediators are prominent in defining macrophage function (26). Bleomycin is an oxygenated iron drug complex used as a chemotherapeutic, which exerts cytotoxicity via DNA cleavage (27). This DNA damage results in epithelial cell death and subsequent tissue damage. This promotes macrophage activation and recruitment to the lung, which, if unresolved, can produce a shift to fibroproliferative signaling (10). *This study is based on the concept that administration of OA-NO_2 can limit the inflammatory response to ITB-mediated lung injury via regidation of pro-inflammatory macrophage activation and recruitment*. We found that OA-NO_2 administration reduced the severity of ALI via preservation of resident alveolar macrophage phenotypes and suppression of interstitial macrophage activation. OA-NO_2 also reduced the fibrotic potential of proliferative mesenchymal cells, indicating the potential for a reduction in fibrosis at later time points.

Methods

Animal Care and Use

All experiments were performed in accordance to Rutgers University IACUC approved protocols conforming to the NIH guidelines for the care and use of laboratory animals. Male wild-type C57BL6/J mice, 6-8 weeks of age (21-26 g), were obtained from Jackson Laboratories (Bar Harbor, ME, USA). Mice were housed in groups of 4 per cage under standard conditions with food and water provided ad libitum. Bleomycin and OA-NO_2 were intratracheally instilled and mice were euthanized 7 d post administration.

OA-NO_2 and Bleomycin Administration

A mixed regioisomer preparation of OA-NO_2 (equimolar 9- and 10-nitro-octadec-9-enoic acid) was synthesized by nitroselenation of oleic acid and purified to >98% (28). Mice were anesthetized with isoflurane and received a single intratracheal installation of either 50 μL PBS, 50 μg OA-NO_2/50 μL PBS (10% DMSO), 3 U/kg bleomycin/50 μL PBS, or 50 μg OA-NO_2/25 μL PBS (10% DMSO) in 3 U/kg bleomycin/25 μL PBS as previously described (10). Mice were observed to ensure the full dose was administered and that mice fully recovered from the isoflurane. 72 hr later, mice were re-anesthetized and intratracheally administered 50 μL PBS or 50 μg OA-NO_2/50 μL PBS (10% DMSO). Mice were euthanized 7 d after initial administration.

Bronchoalveolar Lavage (BAL) Fluid and Lung Cell Collection

Mice were euthanized via a single intraperitoneal injection of ketamine (135 mg/kg) and xylazine (30 mg/kg) (Fort Dodge Animal Health, Fort Dodge, IA). Approximately 5 minutes after injection, depth of the anesthetic was tested by withdrawal from a footpad pinch. Once unresponsive, a thoracotomy was performed and the lungs were perfused with heparin saline via cardiac perfusion. BAL was collected by slowly instilling and withdrawing 5 mL of ice-cold PBS 1mL at a time into the lung through a 20-gauge canula that was inserted into the trachea. BAL was centrifuged for 8 mins at 300 x g and cell pellets were resuspended in

1mL PBS. Cell viability was determined via cell counting with a hemocytometer using trypan blue exclusion dye (ThermoFisher). Supernatant was assessed for protein concentration via a Bradford Protein Assay Kit (Thermo Fisher Scientific) and phospholipid concentrations using the methods of Bligh & Dyer (29).

Histology

After BAL collection, the whole lung was removed and inflation fixed in 2% paraformaldehyde and embedded in paraffin. 5μm sections were then stained with hematoxylin and eosin to observe histological changes. Histological scores were assigned on a 5-point scale adapted from the methods of Beck et al. (30). A score of zero is indicative of no lung injury, meaning there was no airway epithelial thickening, immune cell infiltration, or protein deposition. A score of 5 was indicative of a tissue exhibiting severely thickened airway epithelium, large quantities of infiltrating immune cells, and extensive deposition of proteinaceous debris. Slides were blinded for the assessment of the scorers and scores were statistically analyzed through a Wilcoxon rank-sum test. Slides were assessed using a DP71 microscope (Olympus) at 200x magnification. Whole lung scans were also taken using a VS120 microscope (Olympus).

Lung Tissue Digest

After BAL collection, lung lobes were cut into small pieces and digested in 5 mL of 2 mg/mL collagenase type IV (Thermo Fisher Scientific) in RPMI (Thermo Fisher Scientific) media and 5% FBS (Thermo Fisher Scientific). Tissue was filtered through a 70 μm strainer with RPMI/5% FBS until the strainer was absent of cells. The cells were centrifuged for 6 mins at 400 x g and supernatant was aspirated. Cells were resuspended in 2 mL of Sigma red blood cell lysis buffer for 5 mins at room temperature. 5 mL of RPMI and 5% FBS was added before spinning again at 400xg for 6mins and aspirated. Cells were resuspended in 5 mL of RPMI and 75 μL was removed for flow cytometric analysis. Remaining cells were collected for magnetic separation for single cell western analysis.

Flow Cytometric Analysis

Each sample was brought up to 100μL with staining buffer (PBS+5% FBS+0.02% sodium azide). Samples were incubated with 1μl TruStain FcX™ anti-mouse CD16/32 (Fc block) (BioLegend) for 10mins at 4°C to prevent non-specific binding. Samples were then incubated for 30 mins in the following antibody cocktails (1μL of each). BAL and half of the digested cells were incubated with CD11b, CD206 (MMR), F4/80, CD11c, CD45, Ly-6C, Siglec-F, and MHCII. The other half of the digested cells were incubated with SCA-1, CD45, CD31, CD90, and CD44. Specific antibody details such as conjugation, host species, vendor and catalog number can be found in supplemental figure 1. Cells were washed with staining buffer and incubated with eFluor 780-conjugated fixable viability dye (eBiosciences) for 30 minutes. Cells were washed with staining buffer and fixed in 3% paraformaldehyde. Cells were analyzed using a Beckman Coulter Gallios 10 color flow cytometer (Brea, CA). Cell populations were discerned based on forward and side scatter, doublet discrimination, and viability. Data were analyzed using Beckman Coulter Kaluza flow cytometry software. Antibodies were chosen on the basis of previously published phenotypic marker identifications (Table 1). The gating strategy used for BAL cells,

interstitial cells, and mesenchymal cells are outlined in supplemental figures 1–3. The gating strategy used was adapted from previous publication (31) and is outline in supplemental figures 1–3.

Quantitative RT PCR

After BAL collection, lungs were immediately frozen at −80°C. After thawing, lungs were cut into smaller pieces (approximately 3 mg/piece). Tissues pieces were lysed using Fastprep-24 5G (MP Biomedicals), and diluted in 300 μl of Qiagen buffer RLT (Qiagen) with β-mercaptoethanol (MilliporeSigma). Total RNA was isolated using RNeasy Fibrosis Tissue Mini kit (Qiagen). The RNA quality and concentration were measured using the NanoDrop spectrophotometer (Thermo Fisher Scientific). cDNA was prepared according to iScript (Bio-Rad) instructions using 500 ng purified RNA. Taqman assays were used to analyze relative gene expression using Taqman fast master mix (Thermo Fisher Scientific), Taqman primers: gapdh (Mm99999915_g1, Thermo Fisher Scientific), il6: (Mm99999064_m1, Thermo Fisher Scientific), or nos2 (Mm00440502_ml, Thermo Fisher Scientific), and 25 ng cDNA. Two parallels of each sample were measured separately and results were averaged for statistical analysis.

Tissue Cell CD45 Separation

10^8 cells from tissue digest were resuspended in 1mL of PEF buffer (1xPBS+ 2% FBS+ 1mM EDTA). Cells were incubated with Fc block (Bioledgend) for 5mins at room temperature. CD45 APC antibody (1.5μg/mL, Stem Cell Technologies) was added and cells were incubated at room temperature for 15mins. After this incubation period, the EasySep® APC selection cocktail (110μg/mL, Stem Cell Technologies) was added and cells were incubated for 15mins at room temperature. EasySep® magnetic nanoparticles (50μL/mL, Stem Cell Technologies) were mixed and cells were incubated for 10mins at room temperature. To positively select for CD45 expressing cells, PEF buffer was added to bring samples to 2.5mL and suspension was transferred to 5mL polystyrene tubes. Tubes were placed in an EasyEights™ EasySep™ Magnet (Stem Cell Technologies) and incubated at room temperature for 10 mins. With the tube still in the magnet, supernatant was removed as the first flow through to yield the $CD45^-$ population. The tube was removed from the magnet and wash steps were repeated three times. After the final wash, the tube was removed from the magnet and the cells were resuspended in 2mL PEF buffer, yielding the $CD45^+$ population.

Single Cell Western Blot

After cells were separated into CD45+ and - populations each group was loaded onto a large (6,500 wells) single cell western chip (Protein Simple). The chip was monitored under the microscope until ~50% of the wells were filled and then the chip was run in Milo™ (Protein Simple, San Jose, CA) for 70 seconds. Chips containing CD45− cells were then blocked and incubated with ZEB1 primary antibody (Novus), CD45+ chips were incubated with HMGB1 primary antibody (Proteintech). Chips were then washed and incubated in secondary antibody (Donkey anti-Rabbit IgG (H+L) Highly Cross-Adsorbed Secondary Antibody, Alexa Fluor 647 Thermo Fisher Scientific). Once incubations were complete, chips were

read via a micro-array scanner. Chips were re-probed for β-tubulin (Novus). Micro-array images were analyzed using Scout analysis software (Protein Simple).

Phospholipid and SP-B Analysis

BAL was analyzed for phospholipid using the methodology of Bligh and Dyer (29). SP-B concentrations were measured via western blot using the large aggregate fractions (SP-B) obtained from the phospholipid extraction. Samples of equal phospholipid were loaded onto 4-12% Bis-Tris gels (Thermo Fisher Scientific), transferred to PVDF membranes. The membranes were blocked in 10% non-fat dried milk and 5% TTBS to block non-specific binding and were incubated in SP-B primary antibody (pT3, University of Pennsylvania) overnight and were incubated in Goat-anti-rabbit-HRP secondary antibody (Bio-Rad) before visualization. Bands were analyzed through densitometry via ImageJ software (NIH).

Statistical Analysis

Statistical analysis was performed through SigmaPlot Software. Quantitative data were analyzed by 2-way ANOVA followed by Holm-Sidak test. Qualitative data were analyzed by a Wilcoxon rank-sum test, $p < 0.05$ compared to PBS (*), PBS/OA-NO_2 (#) and bleomycin (†). Quantitative data are expressed as mean ± standard error of the mean and qualitative data are expressed as median and interquartile range [25^{th} percentile, 75^{th} percentile].

Results

OA-NO_2 reduces ITB induced lung injury

ITB administration to mice led to decreased body weight when compared to controls ((44), Fig 1). On average, mice lost 4% (*, $p < 0.05$) of total body weight. This loss was mitigated when mice were administered OA-NO_2 on d0 and d3 (0.82±0.82%, # $p < 0.05$). Moreover, mice given PBS and two doses of OA-NO_2 gained significantly more weight than those given PBS alone.

To characterize lung injury induced by ITB, lung sections were analyzed by histopathology. Whole lung sections were taken to visualize each lobe of the lung and injury was characterized by airway epithelial thickening, septal damage, infiltrating cells, and the presence of proteinaceous debris. Overall staining and a higher magnification (20x) are shown in Figure 2. Damage was scored to quantify the severity of the injury (30). Vehicle control mice had normal lung characteristics with a median histological score of 1 [1,1] (Fig. 2, Fig. 3). These mice had normal airway epithelium and the alveolar space was intact. There was a limited number of infiltrating cells and no proteinaceous debris in the alveolar space. Overall, there were only minimal signs of injury in PBS instilled mice. Mice receiving PBS and OA-NO_2 intratracheally were similar to those instilled with PBS alone based on histological analysis (1 [1,2]; Fig. 2, Fig. 3). Mice administered ITB had abnormal lung characteristics when compared to controls based on histological scoring (5 [5,5], *, $p < 0.05$); Fig. 2, Fig. 3). The airway epithelium was thicker and uneven in appearance when compared with uninjured lung. There was modest septal damage in ITB-treated mice, but the majority of the alveolar space was intact. There were large patches of infiltrating cells throughout the lung and increased infiltrating immune cell numbers induced by ITB. There

was an increase in the amount of proteinaceous debris in the alveolar space throughout the lung when compared to controls. Mice that were administered ITB and OA-NO_2 did not exhibit these abnormalities in the lung to the same degree as ITB alone (3 [2,3.25], #, $p < 0.05$; Fig. 2D, 2H, Fig. 3). Some airways had epithelia that were thickened to the same degree as ITB alone but there were many airways that appeared normal. The airway epithelium had a smooth appearance despite the increased thickness. This is in contrast to the jagged appearance of the epithelium in ITB alone. The alveolar space was intact, with no apparent septal damage. There were some patches of infiltrating cells present throughout the lung but to a lesser degree than ITB alone. This indicates less cellular invasion. In ITB OA-NO_2 mice there was markedly less proteinaceous debris.

OA-NO_2 treatment limits ITB-induced changes in type II cell function

To assess ITB-induced pulmonary edema and protein accumulation in the lung, total BAL protein concentration was assessed via a Bradford assay (Fig. 4). ITB significantly increased protein concentration in the BAL fluid compared to controls (96±40 vs. 432±41.8 pg/mL, *, $p < 0.05$). This increase was not mitigated by OA-NO_2 administration (415±40 μg/mL, $p > 0.05$), with no differences in protein concentrations when comparing PBS instilled mice and those administered PBS and OA-NO_2 (64±41.8 μg/mL, $p > 0.05$).

To characterize type II cell function, phospholipid concentrations were measured in the large aggregate surfactant fraction of the BAL. There was an increase in total phospholipid concentration in the BAL of mice administered ITB when compared to controls (17±9.4μg vs. 57±9.4, *, $p < 0.05$; Fig. 5). Phospholipid concentrations were further increased in mice administered ITB and OA-NO_2 when compared to ITB alone (78±9.4μg, #, $p < 0.05$). There was no significant difference in phospholipid concentration between mice administered PBS and PBS and OA-NO_2.

The large aggregate fraction of the BAL was also used to determine the SP-B concentration as a ratio of total phospholipid (Fig 5). There was an increase in the concentration of SP-B per unit phospholipid in ITB mice when compared to PBS controls ($3x10^6$±$2.4xl0^6$ vs. $9x10^6$±$2.6x10^6$ SPB/unit PL, *, $p < 0.05$). The concentration of SP-B per unit phospholipid was further increased in mice administered ITB and OA-NO_2 when compared to ITB alone ($2x10^7$±$2.6x10^6$ SPB/unit PL, #, $p < 0.05$). There was no significant difference in mice administered PBS and OA-NO_2 when compared to those administered PBS alone.

OA-NO_2 preserves resident alveolar macrophage populations that are reduced following ITB

Alveolar macrophages in the BAL fluid were characterized using flow cytometric analysis. Markers utilized for this analysis are described in table 1. There was a decrease in the percentage of $CD45^+$ alveolar macrophages ($F4/80^+SiglecF^+$) in ITB mice compared to controls (89.35±3.5 vs. 30±3.7%, *, $p < 0.05$; Fig. 6, Top). This was not altered by administration of OA-NO_2 (32±3.7%, $p > 0.05$). There was no change in the percentage of cells considered to be alveolar macrophages when comparing PBS or PBS and OA-NO_2 mice. The small population of cells that were viable and expressed CD45 but did not express either Siglec F or F4/80 are thought to be neutrophils, as many of these cells are also CD11b

$^{+}$. This was confirmed through analysis of cytospins of the BAL fluid. There was an increase in the percentage of these cells in mice administered ITB when compared to PBS (1±6.4 vs. 61±6.8%, *, $p < 0.05$) and OA-NO_2 administration had no impact (56+6.4%, $p > 0.05$). The population of viable, $CD45^{+}F4/80^{+}$Siglec F" cells are interstitial in nature as they are also $Cd11b^{+}$. This population is seen in mice administered ITB but are absent in PBS-treated mice.

The phenotypes of alveolar macrophages were further characterized through their expression of CD11c and CD11b. ITB reduced the percentage of resident alveolar macrophages ($CD11c^{+}CD11b^{-}$) and increased the percentage of macrophages with a more migratory phenotype ($CD11c^{+}CD11b^{+}$) compared to controls (4±2.3 vs. 43±2.4%, *, $p < 0.05$; Fig. 6, Bottom). Though OA-NO_2 administration with ITB still decreased the percentage of resident alveolar macrophages, there were significantly lower proportions and numbers of macrophages expressing a migratory phenotype compared to ITB alone (24±2.4%, #, $p < 0.05$). This indicates a preservation of the resident alveolar macrophage population. There was no change in the percentage of resident alveolar macrophages when comparing PBS control to PBS and OA-NO_2-treated mice.

OA-NO_2 reduces mature interstitial macrophage populations present in ITB injury

In the lung digest, phenotypic changes in the interstitial macrophage population were observed with ITB and with OA-NO_2 administration. There was no significant change in the percentage of interstitial macrophages present in each group regardless of treatment (60±4.6 vs 57±49 vs 66±4.9 vs 51±5.2%, $p > 0.05$). Within the digest, the population of cells that were $CD11c^{+}/CD11b^{+}$, indicating maturity, was significantly increased with ITB compared to controls (59±5.1 vs 23±4.8%, *, $p < 0.05$). This was mitigated by OA-NO_2 administration (43±5.4%, #, $p < 0.05$). There was no difference observed between PBS controls and PBS and OA-NO_2.

Interstitial macrophage phenotypes were further characterized through their expression of Ly6C and mannose receptor (MR). ITB increased the percentage of interstitial macrophages that were $Ly6C^{+}$ when compared to controls (13±3.5 vs. 43±3.7%, *, $p < 0.05$; Fig. 7, Top). This was mitigated by administration of OA-NO_2 (29±4.0%, #, $p < 0.05$). There were no significant changes in the Ly6C+ population when OA-NO_2 was given to PBS mice. The percentage of interstitial macrophages expressing MR also increased with ITB administration (5±3.4 vs. 28±3.6%, *, $p < 0.05$; Fig. 7, Bottom). This increase was not seen to the same degree with OA-NO_2 administration (13±3.8%, #, $p < 0.05$). There was no difference between mice administered PBS and PBS with OA-NO_2.

The inflammatory potential of digested cells was further explored through qPCR analysis of iNOS and IL-6. There was a significant increase in iNOS expression in mice administered ITB (0.7±0.39 vs. 3.2±0.39, *, $p < 0.05$). This was not mitigated by OA-NO_2 treatment (2.8±0.39, #, $p < 0.05$). Analysis of IL-6 revealed a significant increase in expression in ITB mice (0.7±0.31 vs 1.9±0.31, *, $p < 0.05$), which was not significantly reduced by OA-NO_2 (1.5±0.31).

OA-NO_2 reduced the fibroproliferative capacity of proliferating mesenchymal cells

In the digested lung tissue, mesenchymal stem cell phenotypes were characterized through flow cytometric analysis. The population of non-myeloid non-endothelial lung cells ($CD45^-CD31^-$) expressing SCA-1 are considered to be mesenchymal stem cells. ITB decreased this population compared to controls (32±4.7 vs. 12±4.9%, *, $p < 0.05$). This was unchanged with OA-NO_2 administration (20±4.9 vs. 5±5.3%, #, $p < 0.05$). From the mesenchymal stem cell population, phenotypes were further characterized through CD44 and CD90 staining. The mean fluorescence intensity (MFI) (45) for $CD44^+$ cells in PBS mice was unchanged with OA-NO_2 administration (298±53.8 vs. 368±57.0 MFI, $p > 0.05$; Fig. 8, Top). Mice administered ITB had a significantly increased CD44 expression which was suppressed by OA-NO_2 (1111±61* vs. 846±61.0 MFI, #, $p < 0.05$; Fig. 8, Top). There were no significant changes in mesenchymal stem cells expressing CD90 with ITB administration compared to controls and this was not altered by OA-NO_2 (Fig. 8, Bottom).

Macrophage and mesenchymal stem cell population responses

In the digested lung tissue, cell populations were resolved via magnetic separation as myeloid derived ($CD45^+$) or non-myeloid derived ($CD45^-$). Each cell population was analyzed for tubulin via single cell western analysis to determine the number of cells present on the 6,400 well chip and for normalizing cell numbers. Myeloid derived cells were analyzed via single cell western blot for HMGB1, a marker of myeloid cell activation (Fig. 9A). Of all cells on the chip, 49% expressed HMGB1 following ITB administration and subsequent lung digestion, a population that was reduced by more than 50% by OA-NO_2 to a proportion of 21%. Cells from ITB and ITB + OA-NO_2 mice expressed HMGB1 to a greater degree than PBS controls, where only 9% of the population expressed detectable HMGB1. Mice administered PBS and OA-NO_2 had a marked increase in HMGB1 expression compared to PBS alone (21%). With ITB + OA-NO_2 administration there is a leftward shift in the HMGB1 expression profile which indicates that the cells that are expressing HMGB1 express it at a lower relative intensity than ITB alone.

Non-myeloid derived cells were analyzed via ZEB1, a marker of fibrotic potential (Fig. 9B). The population of cells expressing ZEB1 following ITB administration was markedly increased (47.3% vs 0.8%), which was not altered by OA-NO_2 (46.4%). There was also no change in the ZEB1 expression profile upon OA-NO_2 treatment.

Discussion

We report that the administration of OA-NO_2 reduced ITB-induced lung injury as shown by the maintenance of body weight and improved lung histology scores ((Figs 1&2). Also, OA-NO_2 increased surfactant production (Fig. 5) and preserved resident alveolar macrophage numbers within the lung while reducing the activation of interstitial macrophages (Figs 6 & 7). Finally, ITB increased expression of HMGB1 within interstitial macrophages and CD44 in mesenchymal stem cells, both of which are reversed by OA-NO_2 (Figs 8 & 9). *This data indicates that the intratracheal administration of OA-NO2 regulates pulmonary cell inflammatory responses to ITB-induced ALI.*

Consistent with previous ITB-induced ALI models (46–48), mice lost a significant amount of body weight compared to controls. This loss was not observed in ITB mice that also received OA-NO_2, indicative of reduced injury that was confirmed by histological analysis (Fig 2). ITB injury is characterized by an increase in infiltrating cells, thickening of the airway epithelium, and the deposition of proteinaceous debris (9,36,49). This was observed in mice receiving ITB but there was a decrease in proteinaceous debris deposition and cellular infiltration with OA-NO_2 administration (Fig. 2 & 3). A significant limitation to our study is that we used the same mice for lavage and histology. The focus of our study was to establish changes in airway lining and interstitial cell phenotypes and therefore it was necessary to perform lavage to separate these cell populations. We chose not to perform a separate set of animals purely for histology in order to reduce animal usage numbers in alignment with 3Rs principles (50). This obviously means that specific conclusions as to the effects of OA-NO_2 on ITB induced injury drawn from the histology should be treated with caution. In addition, as the lavage procedure can alter cellular processes it is possible that changes in the phenotypes observed are related to different proportions of cellular adhesion.

Another significant limitation of our study was the use of 10% DMSO as the diluent for OA-NO_2. DMSO has anti-oxidant properties itself and has the potential to alter injury in the lung (51,52). However, we have previously found that 10% DMSO does not significantly alter histological score or percent loss of bodyweight (−5±0.2 vs. −6±1.8%) in the ITB model (unpublished observation). This indicates that DMSO does not have a large effect on injury response at the levels used in this experiment. Alternative ways to administer OA-NO_2, without the use of DMSO should still be considered in the future. In this regard, it is interesting to note that OA-NO_2 can be given orally (53) and this may represent an important route of administration in systemic bleomycin injury.

Alveolar macrophages are commonly effected by ITB induced injury (8,23), and we reasoned that OA-NO_2 administered to the lung would reduce macrophage activation in the airspace, due to anti-inflammatory properties (21). Prior work performed by Reddy et al. demonstrated suppression of inflammatory phenotypes in alveolar macrophages by OA-NO_2. These changes were observed in LPS induced ALI and injury brought on via cigarette smoke through cytokine analysis and RT-PCR (18,19). These studies found decreases in several cytokines that are indicative of alveolar macrophage activation when OA-NO_2 was present, indicating that this compound may work to reduce ITB mediated ALI via inhibited alveolar macrophage activation. ITB reduced the relative proportion of BAL $CD45^+$ macrophages, with this reduction not altered by OA-NO_2 (Fig 6). While the number of alveolar macrophages was not significantly lowered by ITB and OA-NO_2, there is an increase in $CD11b^+$ cells that are Siglec F^-. These cells are most likely neutrophils recruited as a result of the injury, as observed in cytospins (not shown), though this data is limited due to a lack of specific neutrophil markers such as Ly6G. This marker was not utilized as neutrophils were not the main focus of our study, but should be considered in future studies. That these cells are present irrelevant of OA-NO_2 administration agrees with protein data, which indicates that OA-NO_2 does not alter the direct epithelial injury resulting from ITB. This indicates that the improvements in outcome mediated by OA-NO_2 result from altered inflammatory signaling.

Altered inflammatory signaling is further indicated by changes in alveolar macrophage phenotypes (Fig 6). Resident alveolar macrophages are $CD11c^{+}CD11b^{-}$, while migratory cells are $CD11b^{+}$ (8,34). The increased $CD11b^{+}$ (migratory) macrophage population following ITB was reduced by OA-NO_2. Irrespective of OA-NO_2 administration, the majority of these $CD11b^{+}$ cells are also $CD11c^{+}$. As CD11c is a marker of lung macrophage maturity, changes in this population may be the result of resident alveolar macrophages becoming more migratory in nature as they begin to express CD11b (54). Alternatively, it may be that interstitial cells are migrating into the alveolar space, where they develop CD11c, becoming more resident in nature (54–56). In any event, OA-NO_2 reduces this migratory activation and may do so by either preserving the resident alveolar macrophage population directly by reducing activation or by reducing recruitment from the interstitium. Signaling targets relevant to OA-NO_2 actions include inhibition of pro-inflammatory NF-κB (21), STATs (57), and MAPK and INK activation (58). Alternatively, the activation of anti-inflammatory signaling such as Keap1/Nrf2 (20) and PPAR-γ-regulated gene expression (22,59) may be critical to the effects of OA-NO_2. This is in agreement with the work of Reddy et al. where it was demonstrated OA-NO_2 reduces NF-κB binding activity and increases Nrf2 and PPAR-γ activity in alveolar macrophages in LPS treated mice (19). This alteration of signal transduction may result in the resident alveolar macrophages maintaining their phenotype rather than expressing CD11b and moving to a more migratory state.

BAL protein content, a marker of edematous epithelial damage and leakage of vascular plasma proteins into airspaces, was increased by ITB. In contrast to other indices of lung injury, increased BAL protein was not reversed by OA-NO_2 (Fig. 4). Protein in the BAL is actual a complex marker as it can be affected by protein secretion from epithelial cells in both the upper and lower airway, as well as from vascular leak. In this regard it is interesting to note that both total phospholipid and SP-B per unit phospholipid are increased by OA-NO_2 in the BAL of ITB treated mice (Fig 5). In addition, SP-B per phospholipid was increased in ITB alone which is in contrast with other studies where researchers saw a decrease in SP-B expression with ITB (60–63). In these studies investigators measured expression by mRNA from lung tissue, which is an indicator of type II cell transcription. The SP-B/phospholipid ratio is dependent upon type II cell surfactant production, recycling, and macrophage uptake (64,65). It is more directly related to surfactant functionality as surfactant proteins can dynamically alter surface tension (66). The increase in SPB and phospholipids, combined with the increased BAL protein, could be attributed to an increase in type II cell function with OA-NO_2 administration (67,68). (67,68). It is possible that increased SP-B/phospholipid ratio correlates with improved function and a decreased work of breathing. In this regard it would be interesting to consider the pressure volume curves via spirometry testing in these mice as it would be predicted that hysteresis would be increased. However, these studies are beyond the scope of the current work.

There was not a change in the total number of interstitial macrophages regardless of ITB or OA-NO_2 administration, which suggests that, as a whole, this population is relatively stable. Possibly, it represents a pool of cells that are able to replenish macrophage numbers in the airway, while being itself regenerated by recruitment from the blood. ITB administration led to an increased expression of Ly6C (Fig. 7), which is a pro-inflammatory marker indicative of acute macrophage activation (32). OA-NO_2 administration reduced ITB-mediated

increases in Ly6C expression, suggesting reduced acute activation. A similar effect was observed when looking at MR, a pro-fibrotic marker (32,69), indicating that activation of macrophages occurs in response to ITB and is limited by OA-NO_2. 7 d post ITB is an intermediate point in the progression of injury, as it occurs at the end of the acute inflammatory phase and the beginning of its resolution. That we see increases in both acute and adaptive activation of macrophages is consistent with this being a transition point in the progression of the pathology. However, it is interesting that OA-NO_2 limits both forms of activation, which indicates that as well as being an anti-inflammatory agent it may also be anti-fibrotic as it limits adaptive activation. One limitation to this data is that the lung digestion was performed after lavage, which has the potential to alter some cell populations slightly. There is also a potential that some of the lavage cells are not removed before digest, however, we tried to control for this by excluding SiglecF+ cells from the analysis.

The interstitial cells are not directly accessible to compounds delivered to the airway and therefore, it was not necessarily predicted that intratracheal delivery of OA-NO_2 would alter activation of these cells. The alterations in interstitial macrophage phenotype we have observed may be caused by direct interaction of OA-NO_2 with interstitial macrophages leading to a change in intracellular signaling and downregulation of inflammatory phenotypes. These changes could also be caused by OA-NO_2 altering alveolar macrophage populations, such that activation signaling to the interstitium is altered. By preserving the resident population, less inflammatory mediators are released (70), leading to a reduction in interstitial cell activation. In this regard, it is important that OA-NO_2 alters expression of the inflammatory marker HMGB1 across the population of interstitial macrophages. HMGB1 is a regulator of macrophage activation and is expressed at low levels in all macrophages (71). Upon stimulation, HMGB1 is released as a danger signal, while synthesis is increased. A single cell western approach showed ITB increased the number of interstitial macrophages that express HMGB1 and that the relative intensity of expression was altered. ITB diminished the number of cells expressing HMGB1 at low levels and increased the number of those cells expressing HMGB1 at a higher level. This was mitigated by OA-NO_2 administration, restoring the low expressing population and reducing the number of cells expressing HMGB1 at a higher intensity (Fig 9). This reduction in high intensity HMGB1 expression is indicative of decreased macrophage activation and the restoration of the low frequency population may indicate cells returning to baseline.

That OA-NO_2 has a significant effect on the interstitium was further confirmed by examining mesenchymal stem cells within the lung tissue. Analysis of mesenchymal stem cell populations revealed an increase in CD44 expression, indicating pro-fibrotic potential with ITB administration (72,73). This increase may be relevant at later timepoints in ITB-induced lung injury, as fibrosis is a common progression. The role of CD44 in ITB mediated injury is unclear as CD44 knockouts have been shown to display both increased injury (74), and reduced inflammation and fibrosis (75) when administered ITB. Using flow cytometry as an indicator of CD44 expression, we are able to observe more subtle changes. ITB increased CD44 expression overall, but it also broadened the distribution of cells. This may represent variable responses in terms of CD44 expression within these cells. CD44 expression was reduced significantly in mice administered OA-NO_2 with ITB. This may result in a decrease in fibrosis at later timepoints, a topic for future study. At the single cell

level there was a large increase in cells expressing ZEB1, a marker of epithelial to mesenchymal transition, in ITB mice (75). This was unexpected at such an acute timepoint and could be an indicator of progression to fibrosis. There was no effect on this expression with OA-NO_2 administration at this acute timepoint, but we may see a change at later timepoints during resolution.

In summary OA-NO_2 limits bleomycin induced acute lung injury, an effect linked with the suppression of alveolar and interstitial macrophage activation and protection of type II cell function. These responses are consistent with OA-NO_2 modulation of inflammatory signaling. Thus, OA-NO_2 may have therapeutic potential as an antifibrotic and anti-inflammatory agent during the progression and resolution of lung injury.

Supplementary Material

Refer to Web version on PubMed Central for supplementary material.

Acknowledgements

NIH-HL086621, Training grant; R01-HL64937 and P01-HL103455. BAF acknowledges an interest in Complexa, Inc. and Creegh Pharmaceuticals, Inc.

Abbreviations:

ALI	Acute lung injury
ITB	intratracheal bleomycin
NO	nitric oxide
OA-NO_2	nitro-oleic fatty acid
Keap1/Nrf2	kelch-like ECH-associated protein 1/nuclear factor (erythroid-derived 2)-like 2
PPAR-γ	peroxisome proliferator-activated receptor gamma
NF-κB	nuclear factor kappa-light-chain-enhancer of activated B cells
JAK/STAT	janus kinase/signal transducer and activator of transcription proteins
STING	stimulator of interferon genes

References

1. Johnson ER, and Matthay MA (2010) Acute lung injury: epidemiology, pathogenesis, and treatment. J Aerosol Med Pulm Drug Deliv 23, 243–252 [PubMed: 20073554]
2. Matthay MA, and Zimmerman GA (2005) Acute lung injury and the acute respiratory distress syndrome: four decades of inquiry into pathogenesis and rational management. Am J Respir Cell Mol Biol 33, 319–327 [PubMed: 16172252]

3. Dowdy DW, Eid MP, Dennison CR, Mendez-Tellez PA, Herridge MS, Guallar E, Pronovost PJ, and Needham DM (2006) Quality of life after acute respiratory distress syndrome: a meta-analysis. Intensive Care Med 32, 1115–1124 [PubMed: 16783553]
4. Rubenfeld GD, Caldwell E, Peabody E, Weaver J, Martin DP, Neff M, Stern EJ, and Hudson LD (2005) Incidence and outcomes of acute lung injury. N Engl J Med 353, 1685–1693 [PubMed: 16236739]
5. Matute-Bello G, Frevert CW, and Martin TR (2008) Animal models of acute lung injury. Am J Physiol Lung Cell Mol Physiol 295, L379–399 [PubMed: 18621912]
6. Moore BB, and Hogaboam CM (2008) Murine models of pulmonary fibrosis. Am J Physiol Lung Cell Mol Physiol 294, L152–160 [PubMed: 17993587]
7. Redente EF, Jacobsen KM, Solomon JJ, Lara AR, Faubel S, Keith RC, Henson PM, Downey GP, and Riches DW (2011) Age and sex dimorphisms contribute to the severity of bleomycin-induced lung injury and fibrosis. Am J Physiol Lung Cell Mol Physiol 301, L510–518 [PubMed: 21743030]
8. Byrne AJ, Maher TM, and Lloyd CM (2016) Pulmonary Macrophages: A New Therapeutic Pathway in Fibrosing Lung Disease? Trends Mol Med 22, 303–316 [PubMed: 26979628]
9. Izbicki G, Segel MJ, Christensen TG, Conner MW, and Breuer R (2002) Time course of bleomycin-induced lung fibrosis. Int J Exp Pathol 83, 111–119 [PubMed: 12383190]
10. Guo C, Atochina-Vasserman E, Abramova H, George B, Manoj V, Scott P, and Gow A (2016) Role of NOS2 in pulmonary injury and repair in response to bleomycin. Free Radic Biol Med 91, 293–301 [PubMed: 26526764]
11. Schopfer FJ, Vitturi DA, Jorkasky DK, and Freeman BA (2018) Nitro-fatty acids: New drug candidates for chronic inflammatory and fibrotic diseases. Nitric Oxide 79, 31–37 [PubMed: 29944935]
12. Ambrozova G, Martiskova H, Koudelka A, Ravekes T, Rudolph TK, Klinke A, Rudolph V, Freeman BA, Woodcock SR, Kubala L, and Pekarova M (2016) Nitro-oleic acid modulates classical and regulatory activation of macrophages and their involvement in pro-fibrotic responses. Free Radic Biol Med 90, 252–260 [PubMed: 26620549]
13. Awwad K, Steinbrink SD, Fromel T, Lill N, Isaak J, Hafner AK, Roos J, Hofmann B, Heide H, Geisslinger G, Steinhilber D, Freeman BA, Maier TJ, and Fleming I (2014) Electrophilic fatty acid species inhibit 5-lipoxygenase and attenuate sepsis-induced pulmonary inflammation. Antioxid Redox Signal 20, 2667–2680 [PubMed: 24206143]
14. Batthyany C, Schopfer FJ, Baker PR, Duran R, Baker LM, Huang Y, Cervenansky C, Branchaud BP, and Freeman BA (2006) Reversible post-translational modification of proteins by nitrated fatty acids in vivo. J Biol Chem 281, 20450–20463 [PubMed: 16682416]
15. Ceaser EK, Moellering DR, Shiva S, Ramachandran A, Landar A, Venkartraman A, Crawford J, Patel R, Dickinson DA, Ulasova E, Ji S, and Darley-Usmar VM (2004) Mechanisms of signal transduction mediated by oxidized lipids: the role of the electrophile-responsive proteome. Biochem Soc Trans 32, 151–155 [PubMed: 14748737]
16. Isom AL, Barnes S, Wilson L, Kirk M, Coward L, and Darley-Usmar V (2004) Modification of Cytochrome c by 4-hydroxy-2-nonenal: evidence for histidine, lysine, and arginine-aldehyde adducts. JAm Soc Mass Spectrom 15, 1136–1147 [PubMed: 15276160]
17. Delmastro-Greenwood M, Freeman BA, and Wendell SG (2014) Redox-dependent anti-inflammatory signaling actions of unsaturated fatty acids. Annu Rev Physiol 76, 79–105 [PubMed: 24161076]
18. Reddy AT, Lakshmi SP, Muchumarri RR, and Reddy RC (2016) Nitrated Fatty Acids Reverse Cigarette Smoke-Induced Alveolar Macrophage Activation and Inhibit Protease Activity via Electrophilic S-Alkylation. PLoS One 11, e0153336 [PubMed: 27119365]
19. Reddy AT, Lakshmi SP, and Reddy RC (2012) The Nitrated Fatty Acid 10-Nitro-oleate Diminishes Severity of LPS-Induced Acute Lung Injury in Mice. PPAR Res 2012, 617063 [PubMed: 22919366]
20. Kansanen E, Kuosmanen SM, Ruotsalainen AK, Hynynen H, and Levonen AL (2017) Nitro-Oleic Acid Regulates Endothelin Signaling in Human Endothelial Cells. Mol Pharmacol 92, 481–490 [PubMed: 28778983]

21. Cui T, Schopfer FJ, Zhang J, Chen K, Ichikawa T, Baker PR, Batthyany C, Chacko BK, Feng X, Patel RP, Agarwal A, Freeman BA, and Chen YE (2006) Nitrated fatty acids: Endogenous anti-inflammatory signaling mediators. J Biol Chem 281, 35686–35698 [PubMed: 16887803]
22. Reddy AT, Lakshmi SP, Kleinhenz JM, Sutliff RL, Hart CM, and Reddy RC (2012) Endothelial cell peroxisome proliferator-activated receptor gamma reduces endotoxemic pulmonary inflammation and injury. J Immunol 189, 5411–5420 [PubMed: 23105142]
23. Reddy AT, Lakshmi SP, Zhang Y, and Reddy RC (2014) Nitrated fatty acids reverse pulmonary fibrosis by dedifferentiating myofibroblasts and promoting collagen uptake by alveolar macrophages. FASEB J 28, 5299–5310 [PubMed: 25252739]
24. Ichikawa T, Zhang J, Chen K, Liu Y, Schopfer FJ, Baker PR, Freeman BA, Chen YE, and Cui T (2008) Nitroalkenes suppress lipopolysaccharide-induced signal transducer and activator of transcription signaling in macrophages: a critical role of mitogen-activated protein kinase phosphatase 1. Endocrinology 149, 4086–4094 [PubMed: 18467446]
25. Hansen AL, Buchan GJ, Ruhl M, Mukai K, Salvatore SR, Ogawa E, Andersen SD, Iversen MB, Thielke AL, Gunderstofte C, Motwani M, Moller CT, Jakobsen AS, Fitzgerald KA, Roos J, Lin R, Maier TJ, Goldbach-Mansky R, Miner CA, Qian W, Miner JJ, Rigby RE, Rehwinkel J, Jakobsen MR, Arai H, Taguchi T, Schopfer FJ, Olagnier D, and Holm CK (2018) Nitro-fatty acids are formed in response to virus infection and are potent inhibitors of STING palmitoylation and signaling. Proceedings of the National Academy of Sciences of the United States of America 115, E7768–E7775 [PubMed: 30061387]
26. Wentker P, Eberhardt M, Dreyer FS, Bertrams W, Cantone M, Griss K, Schmeck B, and Vera J (2017) An Interactive Macrophage Signal Transduction Map Facilitates Comparative Analyses of High-Throughput Data. J Immunol 198, 2191–2201 [PubMed: 28137890]
27. Burger RM, Peisach J, and Horwitz SB (1981) Activated bleomycin. A transient complex of drug, iron, and oxygen that degrades DNA. J Biol Chem 256, 11636–11644 [PubMed: 6170635]
28. Woodcock SR, Bonacci G, Gelhaus SL, and Schopfer FJ (2013) Nitrated fatty acids: synthesis and measurement. Free Radic Biol Med 59, 14–26 [PubMed: 23200809]
29. Bligh EG, and Dyer WJ (1959) A rapid method of total lipid extraction and purification. Can J Biochem Physiol 37, 911–917 [PubMed: 13671378]
30. Beck JM, Liggitt HD, Brunette EN, Fuchs HJ, Shellito JE, and Debs RJ (1991) Reduction in intensity of Pneumocystis carinii pneumonia in mice by aerosol administration of gamma interferon. Infect Immun 59, 3859–3862 [PubMed: 1682252]
31. Yu YR, O'Koren EG, Hotten DF, Kan MJ, Kopin D, Nelson ER, Que L, and Gunn MD (2016) A Protocol for the Comprehensive Flow Cytometric Analysis of Immune Cells in Normal and Inflamed Murine Non-Lymphoid Tissues. PLoS One 11, e0150606 [PubMed: 26938654]
32. Misharin AV, Morales-Nebreda L, Mutlu GM, Budinger GR, and Perlman H (2013) Flow cytometric analysis of macrophages and dendritic cell subsets in the mouse lung. Am J Respir Cell Mol Biol 49, 503–510 [PubMed: 23672262]
33. St-Pierre J, and Ostergaard HL (2013) A role for the protein tyrosine phosphatase CD45 in macrophage adhesion through the regulation of paxillin degradation. PLoS One 8, e71531 [PubMed: 23936270]
34. Byrne AJ, Mathie SA, Gregory LG, and Lloyd CM (2015) Pulmonary macrophages: key players in the innate defence of the airways. Thorax 70, 1189–1196 [PubMed: 26286722]
35. Myones BL, Dalzell JG, Hogg N, and Ross GD (1988) Neutrophil and monocyte cell surface p150,95 has iC3b-receptor (CR4) activity resembling CR3. J Clin Invest 82, 640–651 [PubMed: 2969921]
36. Ji WJ, Ma YQ, Zhou X, Zhang YD, Lu RY, Sun HY, Guo ZZ, Zhang Z, Li YM, and Wei LQ (2014) Temporal and spatial characterization of mononuclear phagocytes in circulating, lung alveolar and interstitial compartments in a mouse model of bleomycin-induced pulmonary injury. J Immunol Methods 403, 7–16 [PubMed: 24280595]
37. Gibbons MA, MacKinnon AC, Ramachandran P, Dhaliwal K, Duffin R, Phythian-Adams AT, van Rooijen N, Haslett C, Howie SE, Simpson AJ, Hirani N, Gauldie J, Iredale JP, Sethi T, and Forbes SJ (2011) Ly6Chi monocytes direct alternatively activated profibrotic macrophage regulation of lung fibrosis. Am J Respir Crit Care Med 184, 569–581 [PubMed: 21680953]

38. Yang J, Zhang L, Yu C, Yang XF, and Wang H (2014) Monocyte and macrophage differentiation: circulation inflammatory monocyte as biomarker for inflammatory diseases. Biomark Res 2, 1 [PubMed: 24398220]
39. Bantikassegn A, Song X, and Politi K (2015) Isolation of epithelial, endothelial, and immune cells from lungs of transgenic mice with oncogene-induced lung adenocarcinomas. Am J Respir Cell Mol Biol 52, 409–417 [PubMed: 25347711]
40. McQualter JL, Brouard N, Williams B, Baird BN, Sims-Lucas S, Yuen K, Nilsson SK, Simmons PJ, and Bertoncello I (2009) Endogenous fibroblastic progenitor cells in the adult mouse lung are highly enriched in the sca-1 positive cell fraction. Stem Cells 27, 623–633 [PubMed: 19074419]
41. Xu H, Tian Y, Yuan X, Wu H, Liu Q, Pestell RG, and Wu K (2015) The role of CD44 in epithelial-mesenchymal transition and cancer development. Onco Targets Ther 8, 3783–3792 [PubMed: 26719706]
42. An Z, Sabalic M, Bloomquist RF, Fowler TE, Streelman T, and Sharpe PT (2018) A quiescent cell population replenishes mesenchymal stem cells to drive accelerated growth in mouse incisors. Nat Commun 9, 378 [PubMed: 29371677]
43. Schaper F, de Leeuw K, Horst G, Bootsma H, Limburg PC, Heeringa P, Bijl M, and Westra J (2016) High mobility group box 1 skews macrophage polarization and negatively influences phagocytosis of apoptotic cells. Rheumatology (Oxford) 55, 2260–2270 [PubMed: 27632996]
44. Barbayianni I, Ninou I, Tzouvelekis A, and Aidinis V (2018) Bleomycin Revisited: A Direct Comparison of the Intratracheal Micro-Spraying and the Oropharyngeal Aspiration Routes of Bleomycin Administration in Mice. Front Med (Lausanne) 5, 269 [PubMed: 30320115]
45. Tanaka Y, Aleksunes LM, Yeager RL, Gyamfi MA, Esterly N, Guo GL, and Klaassen CD (2008) NF-E2-Related Factor 2 Inhibits Lipid Accumulation and Oxidative Stress in Mice Fed a High-Fat Diet. J Pharmacol Exp Ther 325, 655–664 [PubMed: 18281592]
46. Gilhodes JC, Jule Y, Kreuz S, Stierstorfer B, Stiller D, and Wollin L (2017) Quantification of Pulmonary Fibrosis in a Bleomycin Mouse Model Using Automated Histological Image Analysis. PLoS One 12, e0170561 [PubMed: 28107543]
47. Chen ES, Greenlee BM, Wills-Karp M, and Moller DR (2001) Attenuation of lung inflammation and fibrosis in interferon-gamma-deficient mice after intratracheal bleomycin. Am J Respir Cell Mol Biol 24, 545–555 [PubMed: 11350823]
48. Genovese T, Cuzzocrea S, Di Paola R, Mazzon E, Mastruzzo C, Catalano P, Sortino M, Crimi N, Caputi AP, Thiemermann C, and Vancheri C (2005) Effect of rosiglitazone and 15-deoxy-Delta12,14-prostaglandin J2 on bleomycin-induced lung injury. Eur Respir J 25, 225–234 [PubMed: 15684285]
49. Lindenschmidt RC, Tryka AF, Godfrey GA, Frome EL, and Witschi H (1986) Intratracheal versus intravenous administration of bleomycin in mice: acute effects. Toxicol Appl Pharmacol 85, 69–77 [PubMed: 2425458]
50. Smith AJ, and Lilley E (2019) The Role of the Three Rs in Improving the Planning and Reproducibility of Animal Experiments. Animals (Basel) 9
51. Pepin JM, and Langner RO (1985) Effects of dimethyl sulfoxide (DMSO) on bleomycin-induced pulmonary fibrosis. Biochem Pharmacol 34, 2386–2389 [PubMed: 2409982]
52. Haschek WM, Baer KE, and Rutherford JE (1989) Effects of dimethyl sulfoxide (DMSO) on pulmonary fibrosis in rats and mice. Toxicology 54, 197–205 [PubMed: 2466348]
53. Fazzari M, Vitturi DA, Woodcock SR, Salvatore SR, Freeman BA, and Schopfer FJ (2019) Electrophilic fatty acid nitroalkenes are systemically transported and distributed upon esterification to complex lipids. J Lipid Res 60, 388–399 [PubMed: 30545956]
54. Zaynagetdinov R, Sherrill TP, Kendall PL, Segal BH, Weller KP, Tighe RM, and Blackwell TS (2013) Identification of myeloid cell subsets in murine lungs using flow cytometry. Am J Respir Cell Mol Biol 49, 180–189 [PubMed: 23492192]
55. Misharin AV, Morales-Nebreda L, Reyfman PA, Cuda CM, Walter JM, McQuattie-Pimentel AC, Chen CI, Anekalla KR, Joshi N, Williams KJN, Abdala-Valencia H, Yacoub TJ, Chi M, Chiu S, Gonzalez-Gonzalez FJ, Gates K, Lam AP, Nicholson TT, Homan PJ, Soberanes S, Dominguez S, Morgan VK, Saber R, Shaffer A, Hinchcliff M, Marshall SA, Bharat A, Berdnikovs S, Bhorade SM, Bartom ET, Morimoto RI, Balch WE, Sznajder JI, Chandel NS, Mutlu GM, Jain M, Gottardi

CJ, Singer BD, Ridge KM, Bagheri N, Shilatifard A, Budinger GRS, and Perlman H (2017) Monocyte-derived alveolar macrophages drive lung fibrosis and persist in the lung over the life span. J Exp Med 214, 2387–2404 [PubMed: 28694385]

56. Hussell T, and Bell TJ (2014) Alveolar macrophages: plasticity in a tissue-specific context. Nat Rev Immunol 14, 81–93 [PubMed: 24445666]
57. Ambrozova G, Martiskova H, Koudelka A, Ravekes T, Rudolph TK, Klinke A, Rudolph V, Freeman BA, Woodcock SR, Kubala L, and Pekarova M (2016) Nitro-oleic acid modulates classical and regulatory activation of macrophages and their involvement in pro-fibrotic responses. Free Radic Biol Med 90, 252–260 [PubMed: 26620549]
58. Verescakova H, Ambrozova G, Kubala L, Perecko T, Koudelka A, Vasicek O, Rudolph TK, Klinke A, Woodcock SR, Freeman BA, and Pekarova M (2017) Nitro-oleic acid regulates growth factor-induced differentiation of bone marrow-derived macrophages. Free Radic Biol Med 104, 10–19 [PubMed: 28063941]
59. Schopfer FJ, Baker PR, Giles G, Chumley P, Batthyany C, Crawford J, Patel RP, Hogg N, Branchaud BP, Lancaster JR Jr., and Freeman BA (2005) Fatty acid transduction of nitric oxide signaling. Nitrolinoleic acid is a hydrophobically stabilized nitric oxide donor. J Biol Chem 280, 19289–19297 [PubMed: 15764811]
60. Deterding RR, Havill AM, Yano T, Middleton SC, Jacoby CR, Shannon JM, Simonet WS, and Mason RJ (1997) Prevention of bleomycin-induced lung injury in rats by keratinocyte growth factor. Proc Assoc Am Physicians 109, 254–268 [PubMed: 9154642]
61. Savani RC, Godinez RI, Godinez MH, Wentz E, Zaman A, Cui Z, Pooler PM, Guttentag SH, Beers MF, Gonzales LW, and Ballard PL (2001) Respiratory distress after intratracheal bleomycin: selective deficiency of surfactant proteins B and C. Am J Physiol Lung Cell Mol Physiol 281, L685–696 [PubMed: 11504697]
62. Song M, He B, and Qiu Z (1998) [Expression of surfactant protein SP-A, SP-B, and SP-C mRNA in lungs of rats with bleomycin-induced pulmonary fibrosis]. Zhonghua Jie He He Hu Xi Za Zhi 21, 420–422 [PubMed: 11326882]
63. Strayer M, Savani RC, Gonzales LW, Zaman A, Cui Z, Veszelovszky E, Wood E, Ho YS, and Ballard PL (2002) Human surfactant protein B promoter in transgenic mice: temporal, spatial, and stimulus-responsive regulation. Am J Physiol Lung Cell Mol Physiol 282, L394–404 [PubMed: 11839532]
64. Guttentag SH, Beers MF, Bieler BM, and Ballard PL (1998) Surfactant protein B processing in human fetal lung. Am J Physiol 275, L559–566 [PubMed: 9728051]
65. Brasch F, Johnen G, Winn-Brasch A, Guttentag SH, Schmiedl A, Kapp N, Suzuki Y, Muller KM, Richter J, Hawgood S, and Ochs M (2004) Surfactant protein B in type II pneumocytes and intra-alveolar surfactant forms of human lungs. Am J Respir Cell Mol Biol 30, 449–458 [PubMed: 12972403]
66. Cochrane CG, and Revak SD (1991) Pulmonary surfactant protein B (SP-B): structure-function relationships. Science 254, 566–568 [PubMed: 1948032]
67. Whitsett JA, Wert SE, and Weaver TE (2010) Alveolar surfactant homeostasis and the pathogenesis of pulmonary disease. Annu Rev Med 61, 105–119 [PubMed: 19824815]
68. Olajuyin AM, Zhang X, and Ji HL (2019) Alveolar type 2 progenitor cells for lung injury repair. Cell Death Discov 5, 63 [PubMed: 30774991]
69. Liu G, Ma H, Qiu L, Li L, Cao Y, Ma J, and Zhao Y (2011) Phenotypic and functional switch of macrophages induced by regulatory CD4+CD25+ T cells in mice. Immunol Cell Biol 89, 130–142 [PubMed: 20514074]
70. Zhao M, Fernandez LG, Doctor A, Sharma AK, Zarbock A, Tribble CG, Kron IL, and Laubach VE (2006) Alveolar macrophage activation is a key initiation signal for acute lung ischemia-reperfusion injury. Am J Physiol Lung Cell Mol Physiol 291, L1018–1026 [PubMed: 16861385]
71. Xu J, Jiang Y, Wang J, Shi X, Liu Q, Liu Z, Li Y, Scott MJ, Xiao G, Li S, Fan L, Billiar TR, Wilson MA, and Fan J (2014) Macrophage endocytosis of high-mobility group box 1 triggers pyroptosis. Cell Death Differ 21, 1229–1239 [PubMed: 24769733]
72. T LR, Sanchez-Abarca LI, Muntion S, Preciado S, Puig N, Lopez-Ruano G, Hernandez-Hernandez A, Redondo A, Ortega R, Rodriguez C, Sanchez-Guijo F, and del Canizo C (2016) MSC surface

markers (CD44, CD73, and CD90) can identify human MSC-derived extracellular vesicles by conventional flow cytometry. Cell Commun Signal 14, 2 [PubMed: 26754424]

73. Offret G, Aubry JP, and Orsoni-Dupont C (1970) [Red light photography of the fundus oculi as a supplement to fluorescent angiography in the study of choroid tumors]. Arch Ophtalmol Rev Gen Ophtalmol 30, 673–682 [PubMed: 4249894]
74. Li Y, Jiang D, Liang J, Meltzer EB, Gray A, Miura R, Wogensen L, Yamaguchi Y, and Noble PW (2011) Severe lung fibrosis requires an invasive fibroblast phenotype regulated by hyaluronan and CD44. J Exp Med 208, 1459–1471 [PubMed: 21708929]
75. Zhang P, Sun Y, and Ma L (2015) ZEB1: at the crossroads of epithelial-mesenchymal transition, metastasis and therapy resistance. Cell Cycle 14, 481–487 [PubMed: 25607528]

Highlights:

- Administration of nitro-oleic acids reduced bleomycin induced acute lung injury
- Activation of inflammatory macrophages was inhibited via nitrated fatty acids
- Nitrated fatty acids reduce fibrotic potential of proliferating mesenchymal cells
- Single cell western blotting identifies novel cellular populations

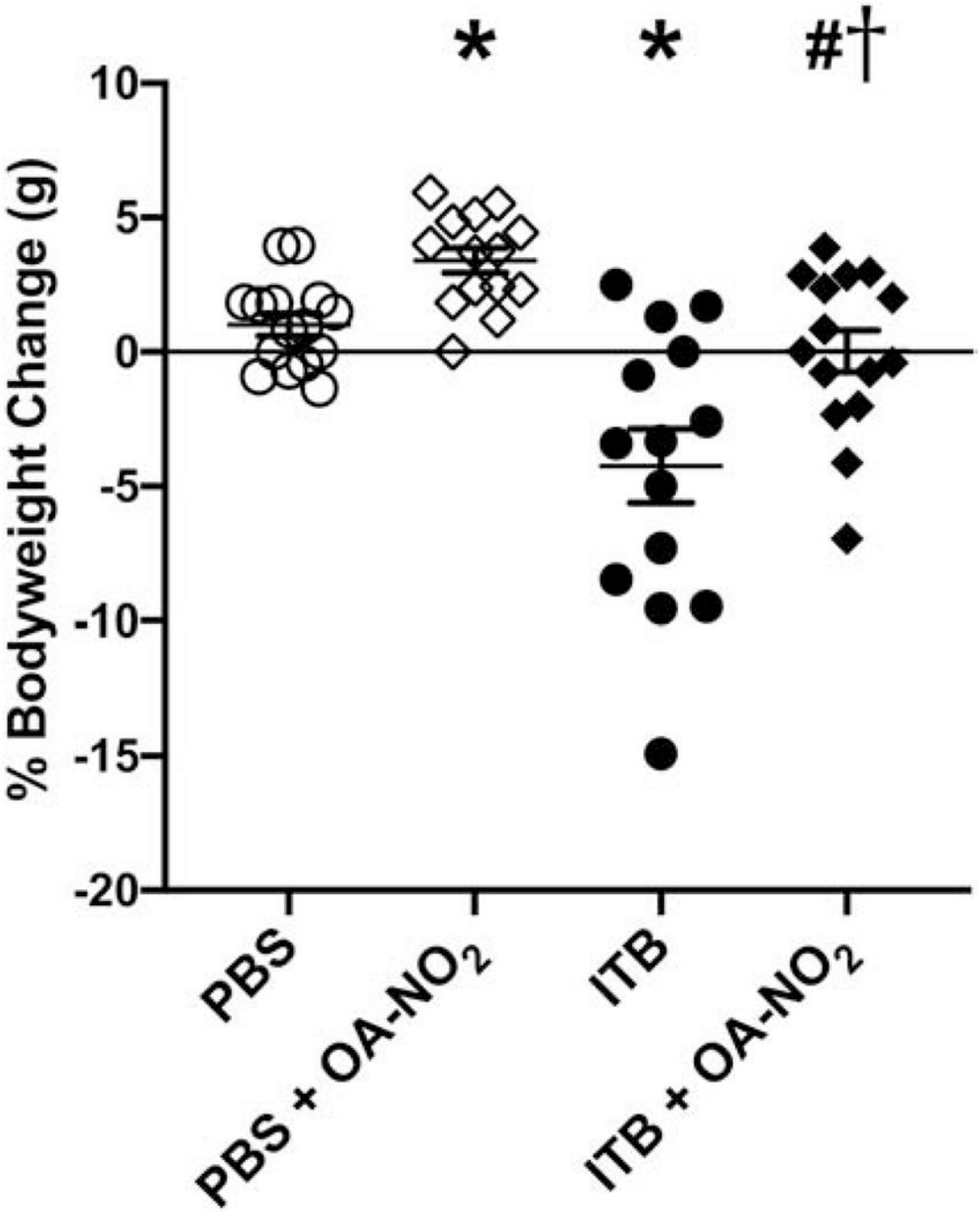

Figure 1.

Intratracheal administration of OA-NO_2 reduces the percent bodyweight lost following ITB. ITB was administered on d0 and OA-NO_2 was administered on d0 and d3. Overall changes in bodyweight were observed on d7. Data are representative of 3 separate experiments with n = 14-15 per group. Values are expressed as mean ± SEM and $p < 0.05$ when compared with PBS (*), PBS & OA-NO_2 (#), and ITB (†).

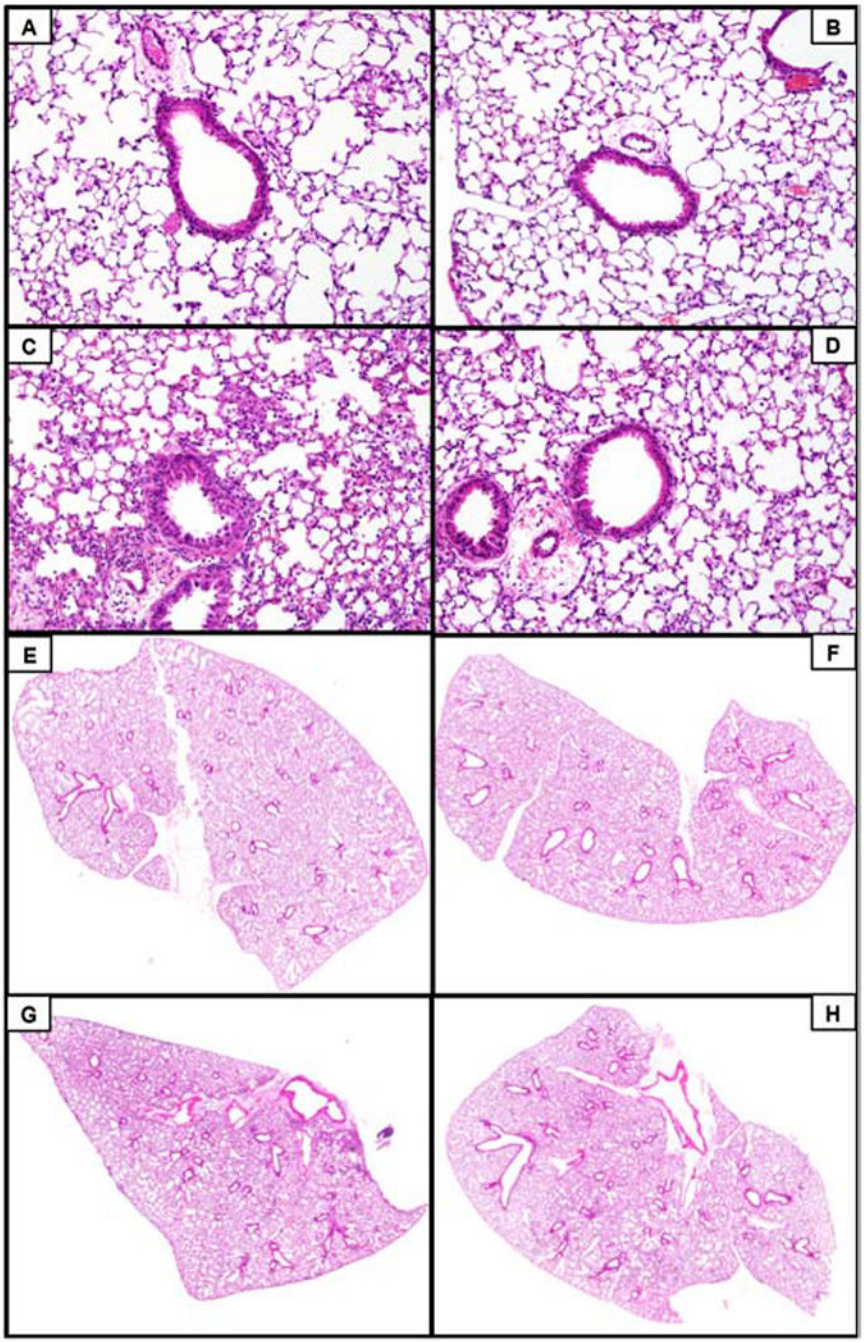

Figure 2.

ITB administration increased the number of infiltrating cells, proteinaceous debris, and airway epithelial thickening, which was mitigated with treatment of OA-NO_2. Lungs were excised 7d following ITB administration and were examined histopathologically via H&E staining. Lung images were taken at 200x. A) PBS, B) PBS and OA-NO_2, C) ITB, and D) ITB and OA-NO_2. The VS 120 microscope was utilized to obtain whole lung images to further observe injury severity, magnification 50x. E) PBS, F) PBS and OA-NO_2, G) ITB,

and H) ITB and OA-NO_2. Data are representative of 3 separate experiments; N=5-6 per group.

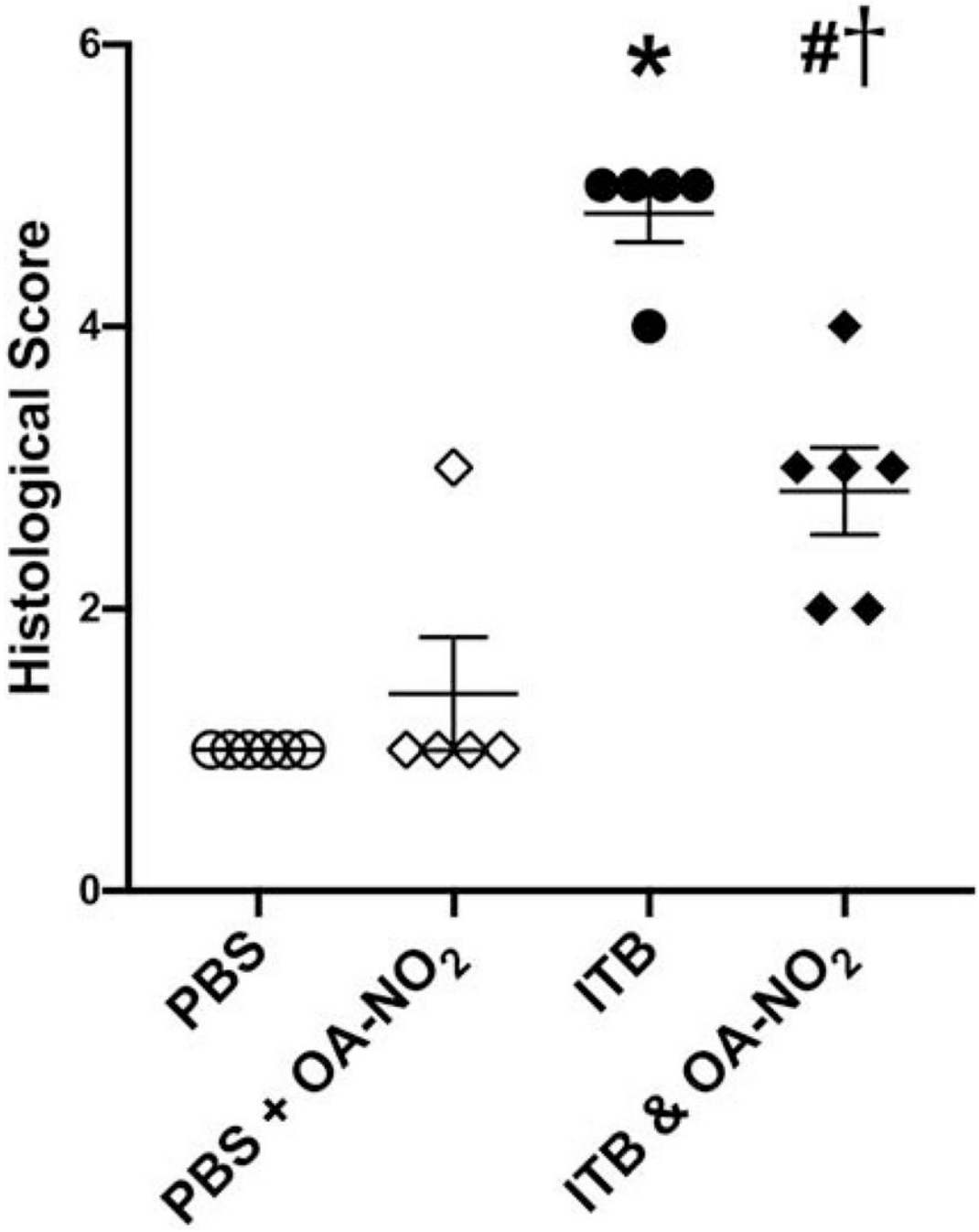

Figure 3.

ITB administration increases injury severity which is mitigated by OA-NO_2 administration. Lungs were excised 7d following ITB administration and were examined histopathologically via H&E staining. Injury severity was assessed through blinded histological slide scoring of stained tissues. Slide pathology was scored on a scale from 0-5 with 5 being the highest injury level. Data are representative of 3 separate experiments; N=5-6 per group. Values are expressed as median and interquartile range and $p < 0.05$ when compared with PBS (*), PBS & OA-NO_2 (#), and ITB (†).

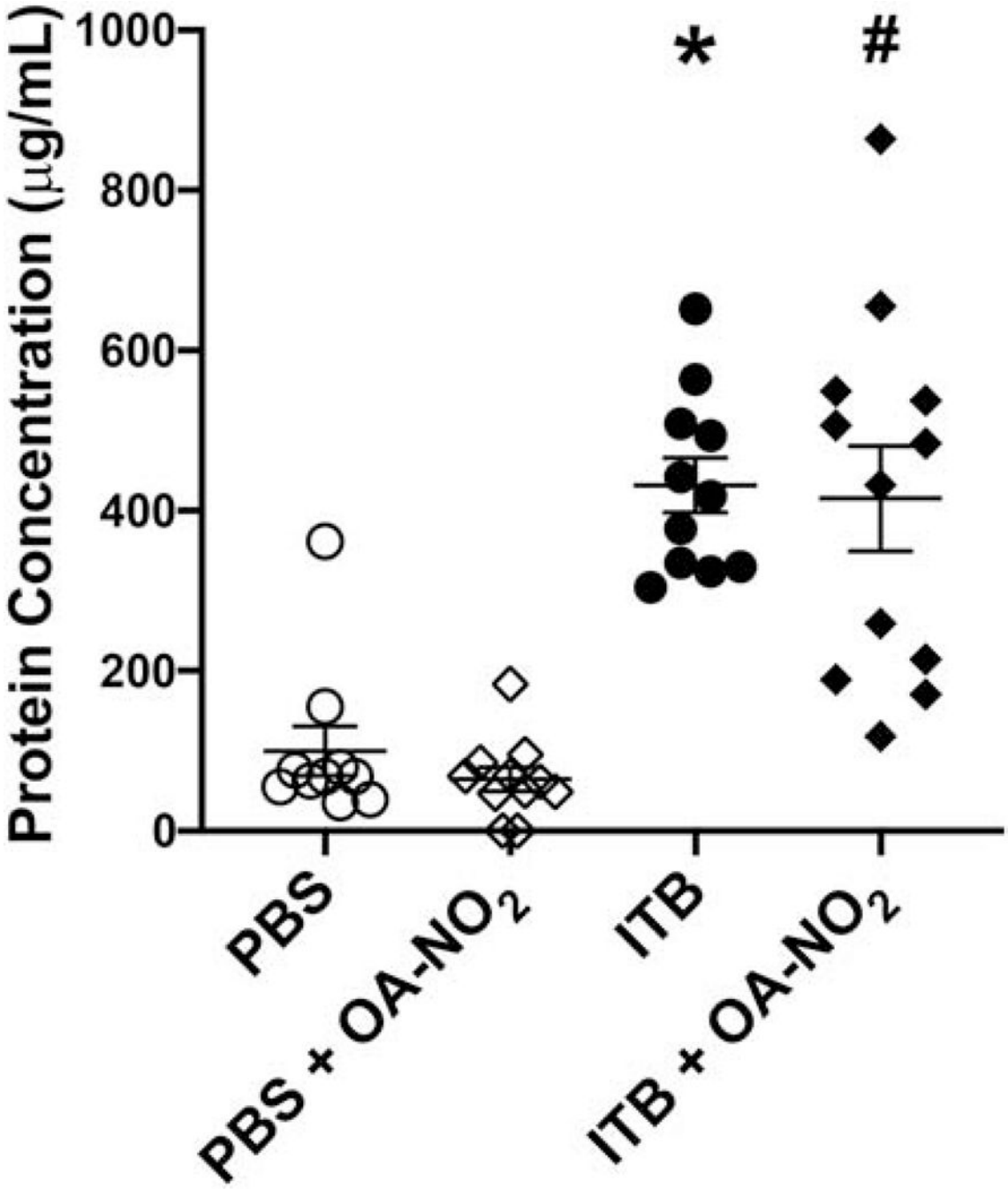

Figure 4.

ITB administration increases the concentration of protein in the BAL and is not altered by OA-NO_2. BAL fluid was obtained 7d post ITB exposure and a Bradford assay was used to determine total protein concentration. Data are representative of 3 separate experiments with n = 14-15 per group. Values are expressed as mean ± SEM and $p < 0.05$ when compared with PBS (*), PBS & OA-NO_2 (#), and ITB (†).

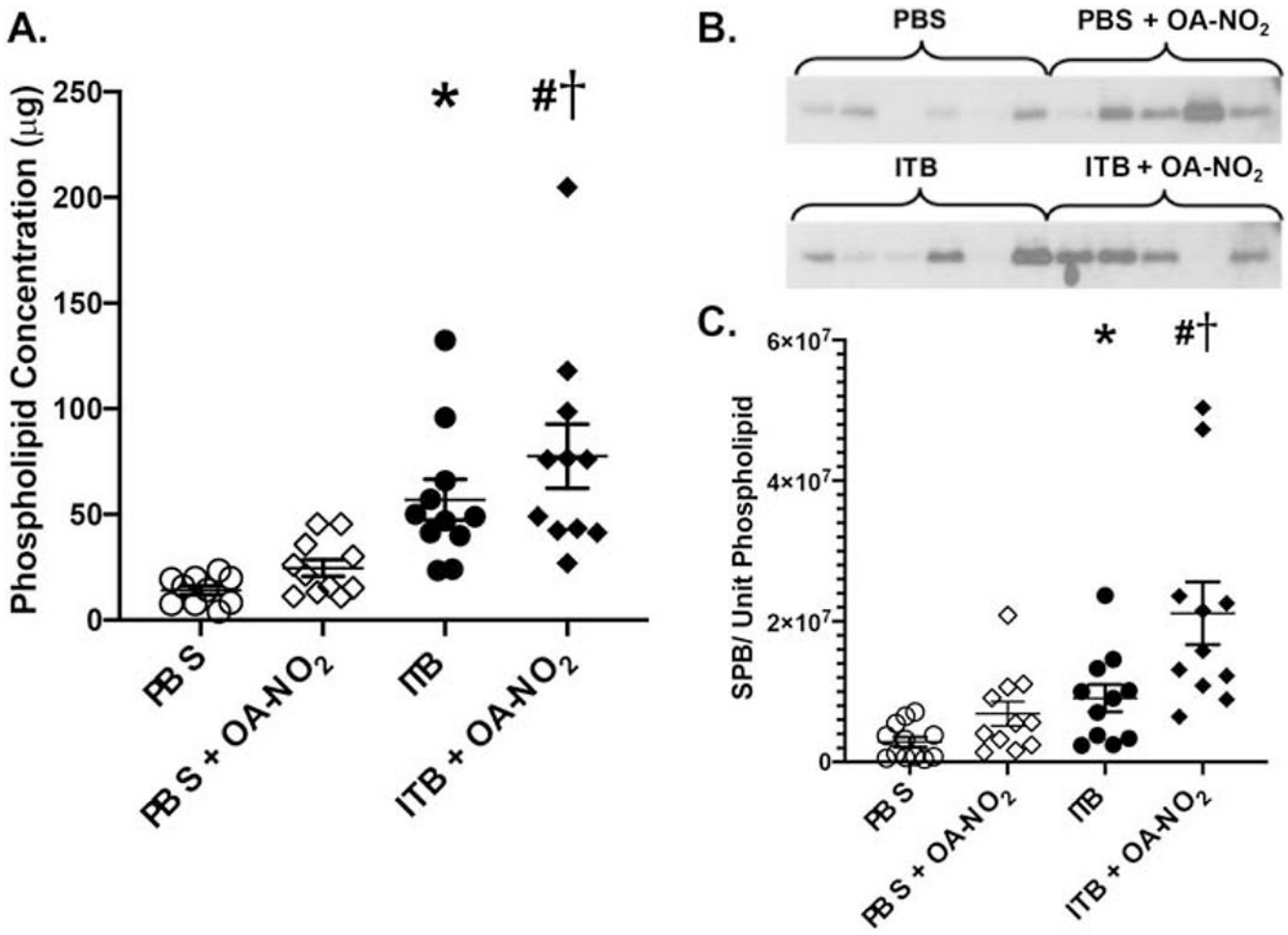

Figure 5.

ITB administration alters the phospholipid concentrations regardless of OA-NO_2. OA-NO_2 administration increases phospholipid and SPB concentrations. Phospholipid concentrations were determined through phospholipid extraction and analysis in the BAL. SPB concentrations were determined through western blot of the large phospholipid aggregate fraction. A) Total phospholipids in the BAL fluid, B) SPB western blot, C) SPB concentration per unit phospholipid densitometry western blot analysis. Data are representative of 3 separate experiments with n = 14-15 per group. Values are expressed as mean ± SEM and $p < 0.05$ when compared with PBS (*), PBS & OA-NO_2 (#), and ITB (†).

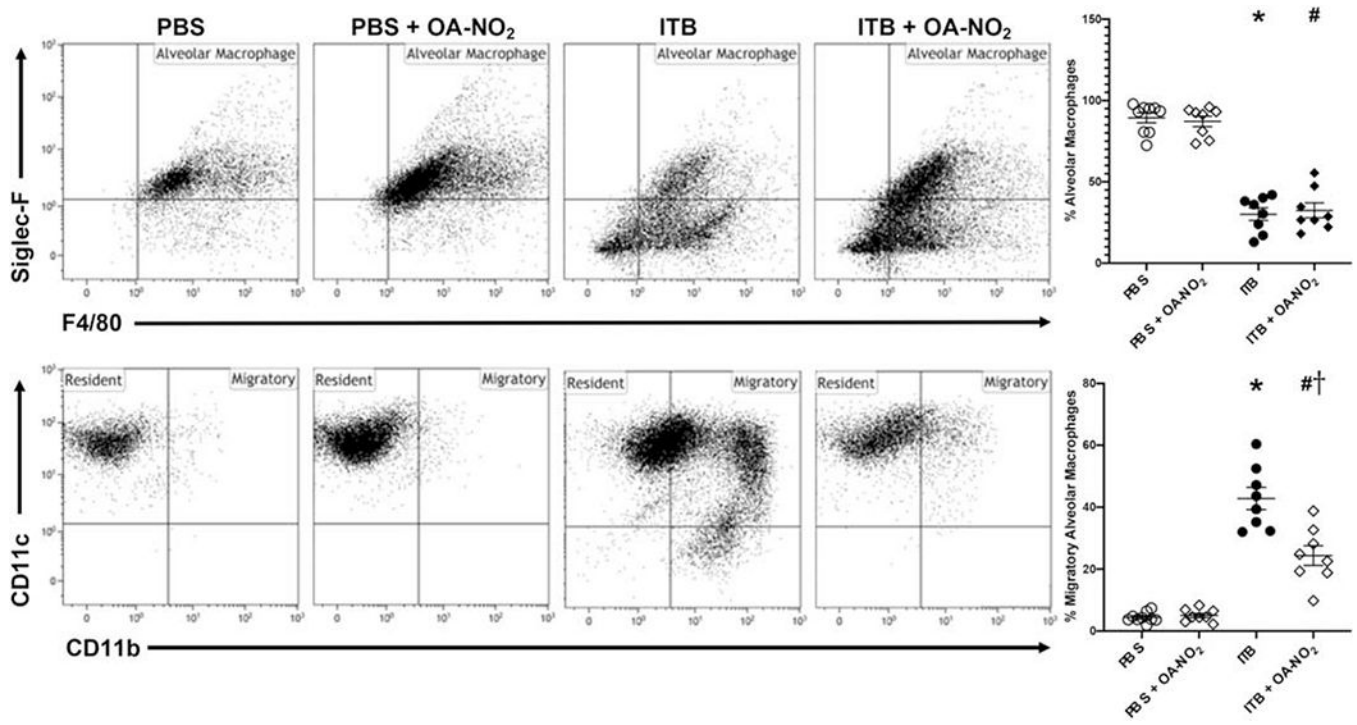

Figure 6.

Flow cytometric analysis of alveolar macrophages. Cells isolated from the BAL 7d after exposure to PBS or ITB with or without OA-NO_2 treatment were immunostained with Siglec F and F4/80 (Top) and CD11c and CD11b (Bottom) as described in the materials and methods. Alveolar macrophages (Siglec F+, F4/80+; top), resident alveolar macrophages (CD11c+, CD11b+; bottom), and migratory alveolar macrophages (CD11c+, CD11b+; bottom) were identified based on forward and side scatter, viability, and CD45+ staining. Data are representative of 2 separate experiments with n = 7-9 per group. Values are expressed as mean ± SEM and $p < 0.05$ when compared with PBS (*), PBS & OA-NO_2 (#), and ITB (†).

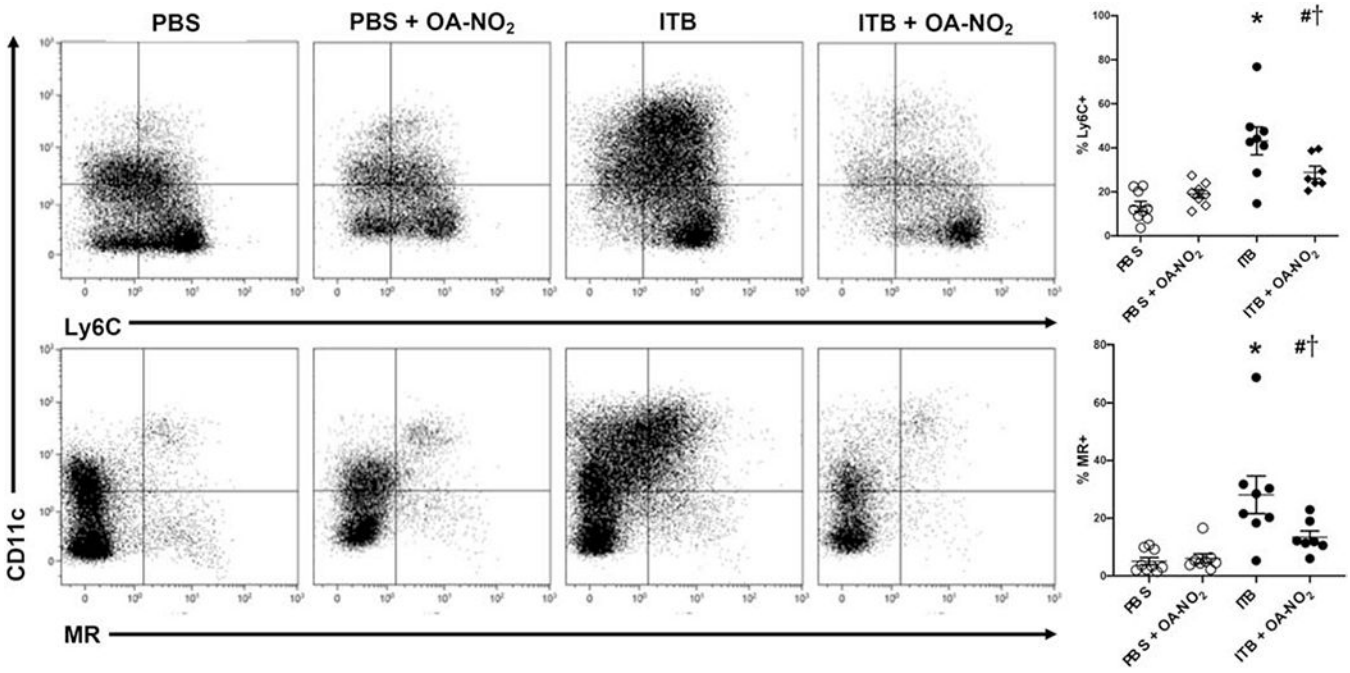

Figure 7.

Flow cytometric analysis of interstitial macrophages. Cells isolated from digested lung tissue 7 d after exposure to PBS or ITB with or without OA-NO_2 treatment were immunostained with Ly6C (middle), and MR (bottom) as described in the materials and methods. Interstitial macrophages were defined as Siglec F^-/$F4/80^+CD11b^+$ and were identified through forward and side scatter, viability, and $CD45^+$ staining. Presence of F4/80 rules out the possibility of these cells being granulocytic. This population was used to visualize Ly6C staining (top) as a marker of acute activation and MR staining (bottom) as a marker of fibrotic activation. Data are representative of 2 separate experiments with n = 7-9 per group. Values are expressed as mean ± SEM and $p < 0.05$ when compared with PBS (*), PBS & OA-NO_2 (#), and ITB (†).

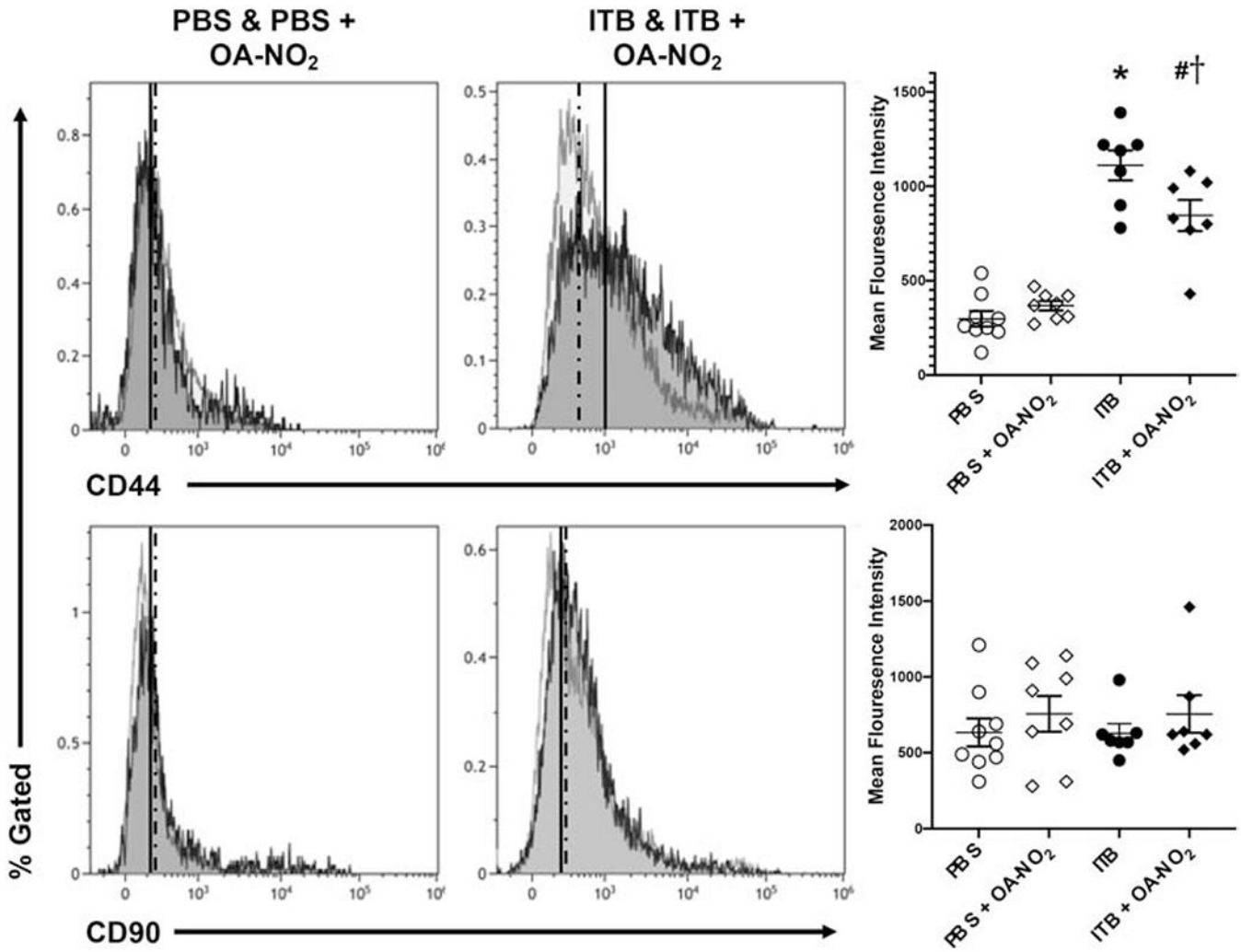

Figure 8.

Flow cytometric analysis of mesenchymal stem cells. Cells isolated from digested lung tissue 7 d after exposure to PBS or ITB with or without OA-NO_2 treatment were immunostained with CD44 and CD90 as described in the materials and methods. Mesenchymal stem cells were defined as $CD31^{-}CD45^{-}SCA\text{-}1^{+}$ and were identified through forward and side scatter and viability. This population was then used to visualize CD44 staining (top) as a marker of pro-fibrotic potential and CD90 staining (bottom) as a marker of proliferative potential. Data are representative of 2 separate experiments with n = 7-9 per group. Values are expressed as mean ± SEM and $p < 0.05$ when compared with PBS (*), PBS & OA-NO_2 (#), and ITB (†).

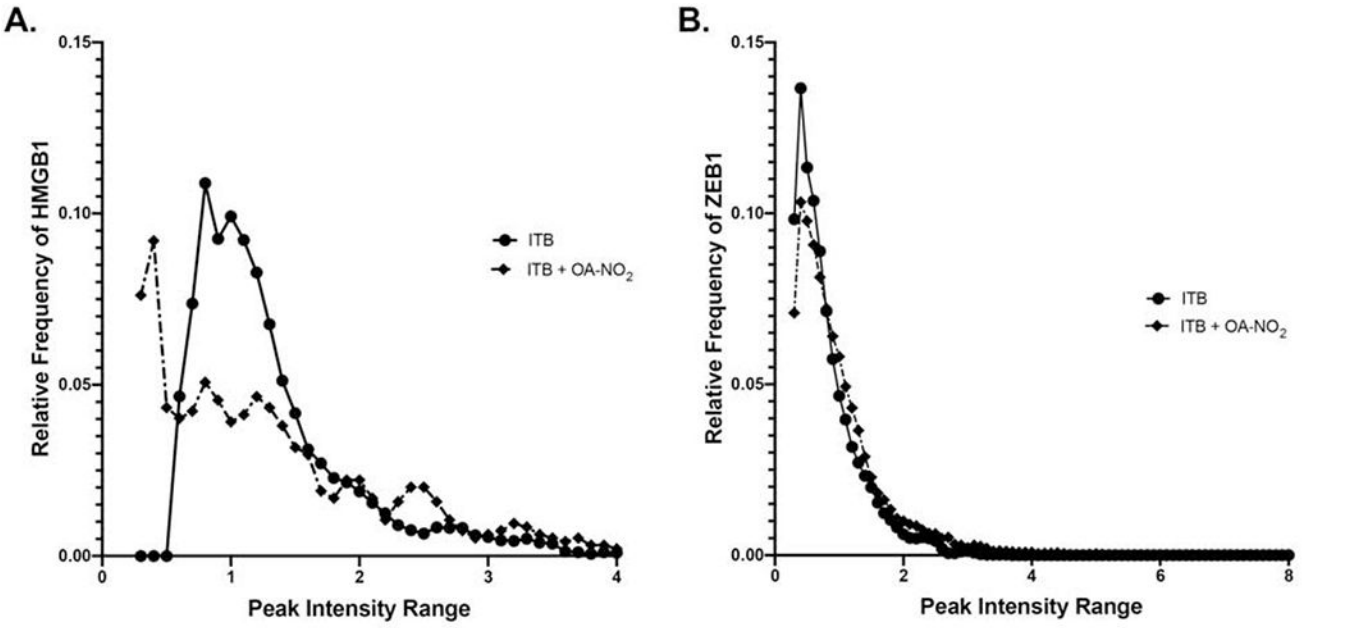

Group	HMGB1+ Cells	Tubulin+ Cells	%Expressing HMGB1
PBS	296	3281	9.0
PBS + OA-NO_2	564	2706	20.8
ITB	2030	4171	48.7
ITB + OA-NO_2	315	1525	20.7

Group	ZEB1+ Cells	Tubulin+ Cells	%Expressing ZEB1
PBS	38	4841	0.8
PBS + OA-NO_2	33	4603	0.7
ITB	2167	4583	47.3
ITB + OA-NO_2	2291	4942	46.4

Figure 9.

Single cell analysis of CD45+ and CD45− cells within lung tissue. Cells isolated from digested lung tissue 7 d after exposure to PBS or ITB with or without OA-NO_2 treatment were separated for CD45+ and CD45− cells as described in the material and methods. Single cell western blotting was utilized to visualize CD45+ cells that were expressing HMGB1 and the relative frequency of cells are expressing at a given intensity (A). HMGB1 is a marker of immune cell activation. This technique was also utilized for CD45− cells to visualize their expression of ZEB1, a marker of epithelial to mesenchymal transition (B). Cells were pooled from 8-9 individual mice and the data is representative of one single cell western chip per group.

Table 1.

Expressional markers used to determine cell populations and characteristics in flowcytometric analysis and single cell western blotting

Marker Name	Expression Profile	Reference
CD45	CD45 is expressed on all myeloid derived cells including interstitial and alveolar macrophages.	(32,33)
Siglec F	Siglec F is highly expressed on alveolar macrophages.	(32)
F4/80	F4/80 is expressed on lung macrophages including both alveolar and interstitial.	(32)
CD11b	CD11b is expressed in interstitial macrophages with lower expression in resident alveolar macrophages. Expression indicates a more migratory phenotype in alveolar macrophages but is characteristic of interstitial macrophages.	(34)
CD11c	CD11c is expressed on resident alveolar macrophages and is a marker of mature interstitial macrophages	(34,35)
MR (CD206)	MR is a profibrotic marker expressed on activated interstitial macrophages. It may also be expressed on alveolar macrophages, indicating M2 polarization.	(32,36)
Ly6C	Ly6C is a pro-inflammatory marker expressed on activated interstitial macrophages, eventually contributing to fibrosis. This marker may also be expressed on alveolar macrophages in a similar manner.	(37,38)
CD31	CD31 is an endothelial cell marker	(39)
SCA-1	SCA-1 is expressed on cells expressing stem cell like characteristics	(40)
CD44	CD44 is expressed on cells undergoing epithelial to mesenchymal transition leading to a pro-fibrotic phenotype	(41)
CD90	CD90 is a marker of proliferation that is expressed on mesenchymal stem cells	(42)
HMGB1	HMGB1 is a pro-inflammatory marker expressed on activated pulmonary macrophages, indicating active inflammation	(43)
ZEB-1	ZEB-1 is a pro-fibrotic marker involved in epithelial to mesenchymal transition and is indicative of fibrosis	(41)